

# **Human vs. Computer: Can we teach the computer to read residual plots?**

A thesis submitted for the degree of

Master

by

Shuofan Zhang

Master, Monash University



Department of Econometrics and Business Statistics

Monash University

Australia

June 2018

# Contents

<b>Acknowledgements</b>	<b>iii</b>
<b>Declaration</b>	<b>v</b>
<b>Abstract</b>	<b>vii</b>
<b>1 Introduction and literature review</b>	<b>1</b>
1.1 Lineup protocol . . . . .	3
1.2 Computer vision . . . . .	4
1.3 Comparing human vs. computer . . . . .	7
<b>2 Comparing computer performance against the database of human evaluation</b>	<b>9</b>
2.1 Amazon Mechanical Turk study . . . . .	9
2.2 Linear relationship simulation . . . . .	12
2.3 Null plot simulation . . . . .	15
2.4 Computer model . . . . .	18
2.5 Comparing results . . . . .	22
2.6 Aside discussion . . . . .	23
<b>3 New experiment comparing human vs. computer on reading heteroskedasticity</b>	<b>25</b>
3.1 A new human experiment . . . . .	26
3.2 Heteroskedasticity simulation . . . . .	27
3.3 Null plot simulation . . . . .	29
3.4 White test . . . . .	30
3.5 Computer model . . . . .	30
3.6 Comparing results . . . . .	32
3.7 Aside discussion . . . . .	32
<b>4 Conclusion and discussion</b>	<b>35</b>
<b>Bibliography</b>	<b>37</b>

# Acknowledgements

I would like to thank my supervisor, Di, for being patient with me as always.

This thesis was written using R markdown with relevant code and data accessible with the text.

<https://github.com/shuofan18/ETF5550>

Software used to conduct this research is R (R Core Team, 2013), Keras (Chollet et al., 2015), ggplot2 (Wickham, 2009)



# **Declaration**

I hereby declare that this thesis contains no material which has been accepted for the award of any other degree or diploma in any university or equivalent institution, and that, to the best of my knowledge and belief, this thesis contains no material previously published or written by another person, except where due reference is made in the text of the thesis.

Shuofan Zhang



# **Abstract**

Residuals plots are a primary means to diagnose statistical models. It requires human evaluation to determine if structure in the plot is consistent with random variation or not. If not, then the diagnosis is that the model has not adequately captured the relationships between response and explanatory variable in the data. This thesis develops a computer vision model to read residual plots. It compares results with a large database of human evaluations. The evaluations were conducted using a protocol called the “lineup” which places residual plots in a formal framework for statistical hypothesis testing. The comparison between computer and human is made on a very restricted and controlled set of residual plot structures. A new small human subject study is also conducted to compare human vs. computer in reading heteroscedasticity.



# **Chapter 1**

## **Introduction and literature review**

“The multiple regression model for cross-sectional data is still the most widely used vehicle for empirical analysis in economics and other social sciences” (Wooldridge, 2015). Detecting possible violations of the Gauss-Markov assumptions is crucial to interpreting the data properly, especially in the early stage of analysis. There are several distribution tests that are commonly used, for instance, the Pearson correlation test for detecting linear relationship; the Breusch-Pagan test and White test for investigating heteroskedasticity. But primarily residual plots are the main diagnostic tool and these rely on human evaluation. Because data plots show a lot more information than a single statistic. A good example here would be Anscombe’s Quartet. “It is a set of four distinct data sets each consisting of 11 (x,y) pairs where each dataset produces the same summary statistics (mean, standard deviation, and correlation) while producing vastly different plots” (Anscombe, 1973). Matejka and Fitzmaurice also did an interesting study on this issue, they used ‘datasaurus’ data from Cairo (2016) and generated a series of data with same statistics but very different plots as shown in figure 1.1. (Matejka and Fitzmaurice, 2017)

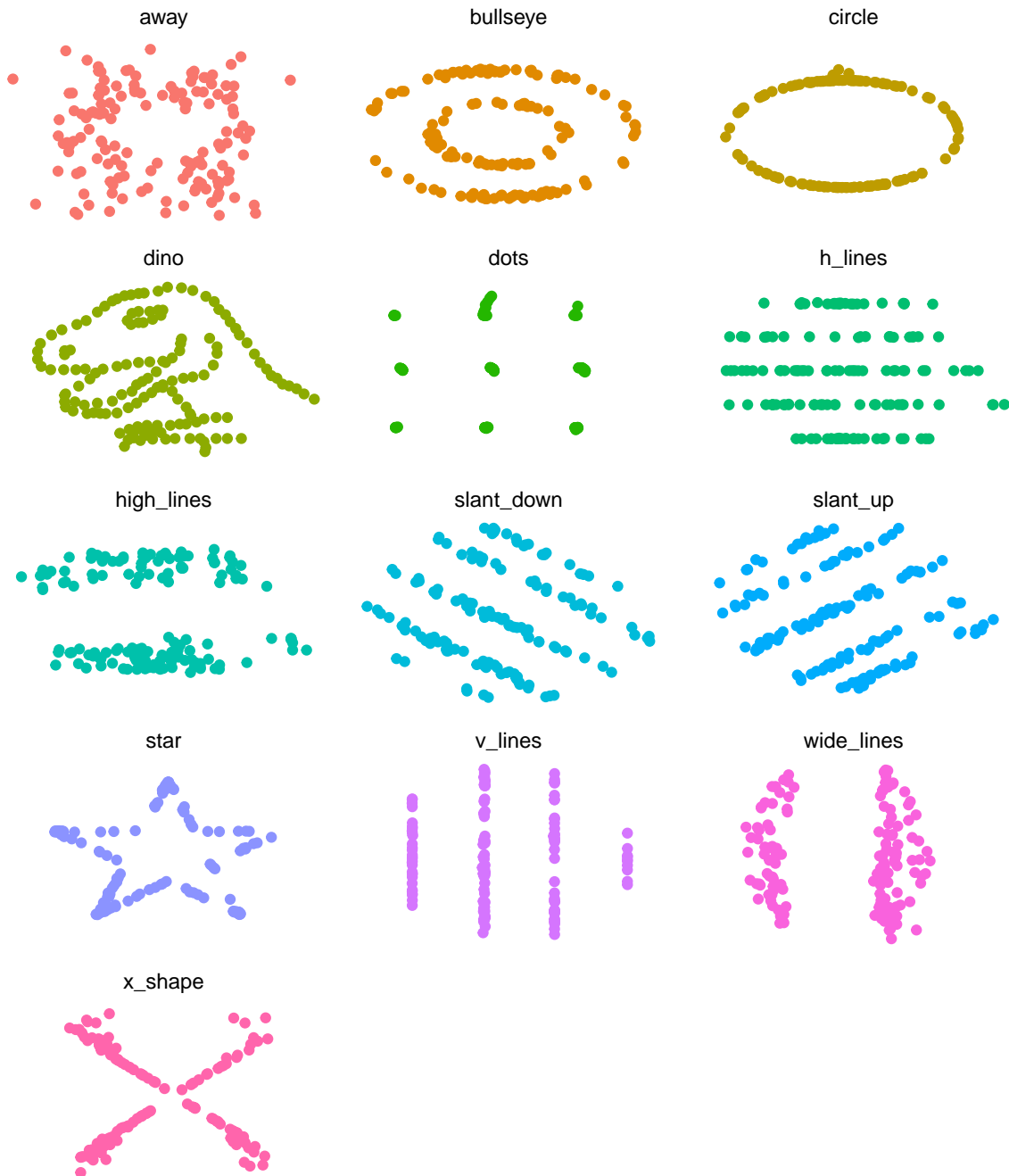


**Figure 1.1:** Each dataset has the same summary statistics to two decimal places: ( $E(x)=54.26$ ,  $E(y)=47.83$ , Pearson's  $r=$ ,  $sd(x)=16.76$ ,  $sd(y)=26.93$ )

## 1.1 Lineup protocol

Former studies have shown that human eyes are sensitive to the systematic patterns in data plots. With proper manipulation, visualized plots can be used as test statistics and perform valid hypothesis test. One example of these protocols that provides inferential validity is called “lineup” which is introduced by Wickham et al. (2010). “The protocol consists of generating 19 null plots (could be other numbers), inserting the plot of the real data in a random location among the null plots and asking the human viewer to single out one of the 20 plots as most different from the others” (Wickham et al., 2010). If the real plot is chosen, it means the real data is likely to be different from the null hypothesis, so we reject the null hypothesis with 5% chance to be wrong (Type I error). Because if all 20 plots are generated from the null distribution, the chance of one plot being picked is  $1/20$  which is 5%. With the assistance of “lineup”, we avoid falling into the trap of apophenia where we see patterns in random noise. This protocol has proved to be valid and powerful theoretically as well as practically through human experiments, especially when the assumptions for doing conventional tests are violated (Majumder, Hofmann, and Cook, 2013). The human factors that may influence visual statistical inference were also investigated by Majumder, Hofmann, and Cook (2014). The experiments in Majumder, Hofmann, and Cook (2014) suggest that “individual skills vary substantially, but demographics do not have a huge effect on performance.” Although there are some statistically significant factors such as “having a graduate degree” and “living country”, the effects of these factors are minimal. These results demonstrate the robustness of the test against different human factors. Figure 1.2 is an example of the lineup. Which plot do you think is the most different? If you choose plot one, we are 95% confident to reject the no-relationship assumption between the two variables, “hp” and “disp” (Simchoni, 2018). The lineup protocol can also be used for other types of testing by choosing different types of plot. For example, normality can be tested using QQ plot; the difference in mean can be tested using box plot; etc.

The question that arises today is whether we can train a computer to read residual plot and make relevant decisions, particularly with a computer vision approach such as deep learning. If this is feasible, we can have the deep learning model process a lot more data

---

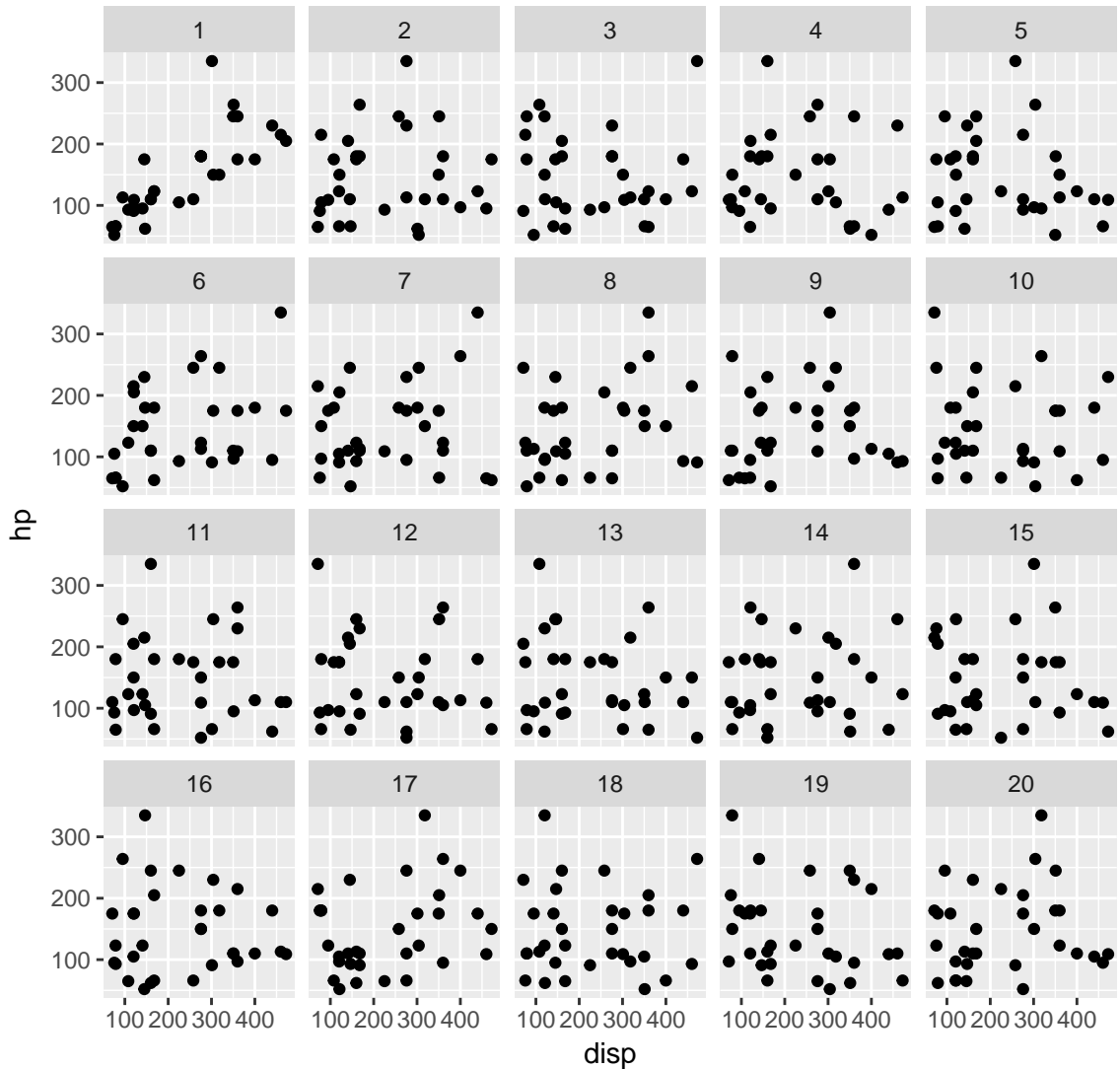


**Figure 1.2:** Scatterplot lineup example: one plot is the data, the rest are generated from a null model assuming no relationship between the two variables. In this lineup it is easy to see that plot 1, which is the data plot, is different from the rest.

than a human can manage. Thus, the cost of rendering visual inference will become much lower.

## 1.2 Computer vision

The motivation for the task is provided in a blog post by Giora Simchoni (Simchoni, 2018). He has designed a deep learning model to test the significance of linear relationship between two variables for samples of size 50. The model reached over 93% accuracy on unseen test data. He also mentioned that the computer fails to pick up a strong non-linear relationship even though the Pearson's r is as high as -0.84 (Simchoni, 2018). So the short

conclusion is the computer vision is not perfect, in that it is not as flexible as human vision. As Simchoni explained in his article, the model can only distinguish linear relationship from no-relationship as trained. However, we think this fact is just another example reflecting the importance of visualization as we discussed above. Strong correlation does not necessarily mean linear relationship. We should always refer to the plot before making any statement. What's more, if we want the model to be more flexible, we could simply adjust our design of training accordingly. Therefore, in this article, we are trying to further Simchoni's study. More specifically, we will build two computer models to perform two hypothesis tests as follows. The first hypothesis test is:

$H_0$ : There are no relationships between the two variables.

$H_1$ : There is a linear relationship between the two variables where all Gauss-Markov assumptions are met.

The second hypothesis test is:

$H_0$ : There is a linear relationship between the two variables where all Gauss-Markov assumptions are met.

$H_1$ : There is a linear relationship between the two variables where the variance of the error term is not a constant while all other Gauss-Markov assumptions are met.

For ease of exposition, only the regression model with one explanatory variable will be considered in this paper, but many of the results can be generalized to other cases including multiple regression model. Because the “statistics” we will use is scatter plot, in terms of teaching the computer reading the plot, one variable is enough to generate different patterns in that plot for convnets to learn. And this makes the design process much simpler.

The model we will use is the convolutional neural networks, also known as convnets, a type of deep-learning model “almost universally used in computer vision applications” (Chollet and Allaire, 2018). The very first convolutional neural networks, called the “LeNet5” which was born in 1994, propelled the field of deep learning. However, this technique was in incubation from 1998 to 2010. In recent years, with the increasing data

---

availability and more advanced technology, the design of the neural network architecture became more and more successful. Many types of neural network architectures have been developed since then, such as the “Dan Ciresan Net” which enabled the implementation of GPU for the first time, and the “AlexNet” which used the so-called “ReLU” function as the activation function and started a small revolution in the deep learning world, etc. (Culurciello, 2017) Basically convolutional neural networks has two interesting properties: “the patterns they learn are translation invariant”, and “they can learn spatial hierarchies of patterns” (Chollet and Allaire, 2018). The first property implies that once the model learns how to recognize linear/heteroskedasticity patterns, it can detect those patterns regardless of their direction, thus handling negative/positive relationship automatically in our case.

Unlike the classical programming where human input rules, in deep learning paradigm, we provide data and the answers associated with the data. Deep learning algorithm will output the rules, and these rules can then be used on new data to make predictions. To make our life easier, we can also think of the deep learning neural network as a complex nonlinear model which could estimate millions of parameters ( $w$ ) with a big enough dataset. As usual regression problem, to get the estimates of unknown parameters ( $w$ ), we need to provide the model with dependent variable ( $y_i$ ) and independent variables ( $x_i$ ). In this case, the independent variable will be the images of data plots (in forms of matrices) simulated from the null distribution and the alternative distribution, and dependent variable will be the labels of that plot indicating the true relationship of the original data. Once we have the estimated parameters ( $\hat{w}$ ), we then can use them to classify unseen data plots, e.g. to perform hypothesis test.

The architecture used in this study is a fundamental one. The estimation method for the deep-learning model is called “backpropagation” algorithm which “is a way to train chains of parametric operations using gradient-descent optimization”. (Chollet and Allaire, 2018) The gradient-descent optimizer is meant to find the set of parameters such that the cost function reaches its minimum. The form of the cost functions or loss function is determined per each question. In both two experiments conducted in this paper, the deep learning model is expected to complete binary classification task, e.g. tell “linearly correlated”

---

variables from “independent” variables for the first experiment, tell “heteroskedasticity errors” from “normal errors” for the second experiment. As introduced by Chollet and Allaire (2018), “crossentropy is usually the best choice (as the loss function) when you’re dealing with models that output probabilities”. Originated from Information Theory, crossentropy is a quantity measuring the distance between probability distributions. In deep learning world, it measures the distance between the true distribution and the predictions. Therefore, in this paper, the binary crossentropy loss function will be used. The associated cost function is of the form,

$$J(\mathbf{w}) = -\frac{1}{N} \sum_{i=1}^N (y_i \log \hat{y}_i + (1 - y_i) \log(1 - \hat{y}_i))$$

where  $\hat{y}_i = g(\mathbf{w} \times \mathbf{x}_i) = \frac{1}{1+e^{-\mathbf{w} \times \mathbf{x}_i}}$  and  $g(z)$  is the logistic function.

### 1.3 Comparing human vs. computer

The main procedures involved in constructing and selecting a convnets model is shown in figure 1.3. The convnets will be trained on “train” and “validation” set. A certain number of iterations over all samples will be done, the fitted convnets given by each iteration will be saved, one best model will be chosen as the representative for the computer according to the overall accuracy on the unseen “test” set.

The main procedures of the human evaluating lineup are given in figure 1.4. “Real data” and “null data” stand for datasets simulated under the alternative hypothesis and the null hypothesis respectively. More detailed procedures related to each hypothesis test will be described in chapter 2 and chapter 3.

Chapter 2 will compare computer performance against the database of human evaluation in reading linear relationship. Steps of constructing computer experiment will be discussed, Turk’s study will be explained, the comparison results will be given. Chapter 3 will compare computer performance against the results from the new human subject study. Details of this new human subject study will be provided. The comparing results will also be presented. Chapter 4 contains a short summary and some discussion regarding to the future study.

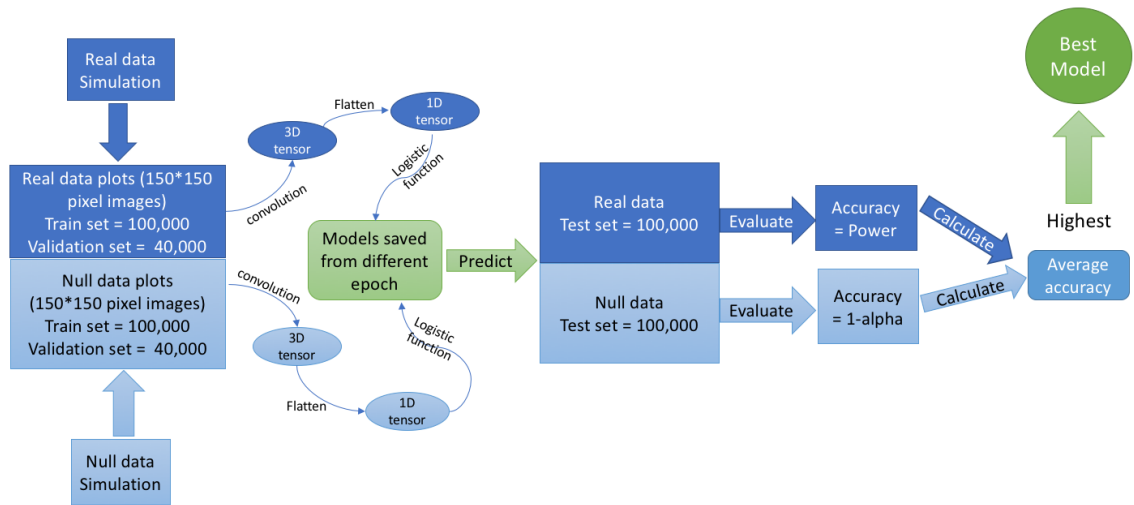


**Figure 1.3:** Diagram illustrating the training, diagnosis and choice of the computer model. Based on 480,000 simulated data sets used to create 150 × 150 pixel images, divided into train, validation and test sets.

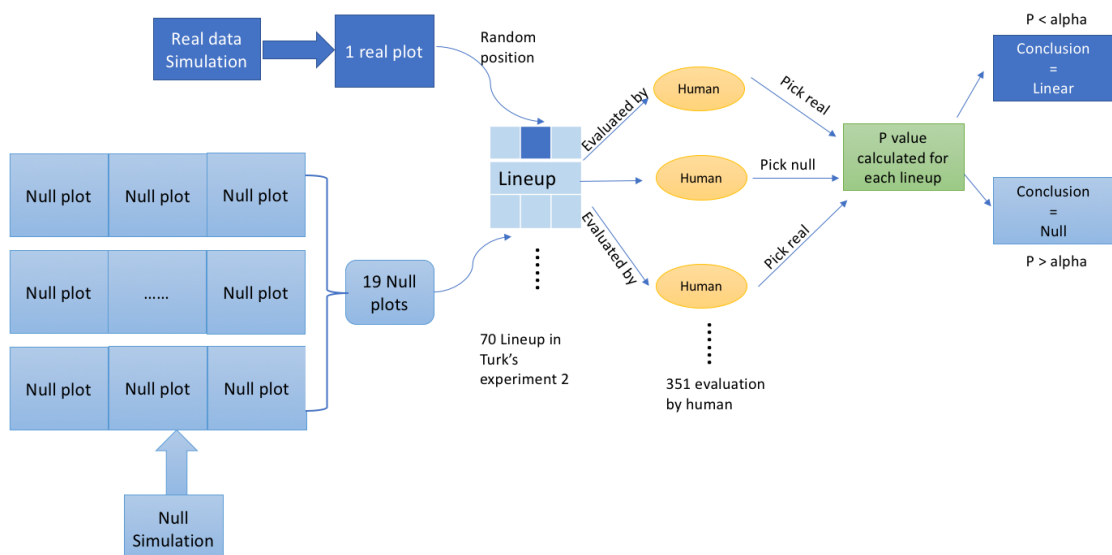


**Figure 1.4:** Diagram illustrating the process of human subject evaluation of lineups, and how performance is computed.

## **Chapter 2**

# **Comparing computer performance against the database of human evaluation**

A database of human evaluations of scatterplots is available from prior studies. This is used to compare the performance of the computer model. The computer model is trained on a broader parameter simulation framework and tested on the same data as the human evaluations.

### **2.1 Amazon Mechanical Turk study**

A large database of results from human subjects was collected examine the performance of the lineup protocol relative to classical tests. The work is published in Majumder, Hofmann, and Cook (2013). This database forms the basis of the test set used to examine the computer model performance.

In Majumder, Hofmann, and Cook (2013), “three experiments were conducted to evaluate the effectiveness of the lineup protocol relative to the equivalent test statistic used in the regression setting.” In each experiment, they simulated data from a controlled setting and then generated associated lineup for the human to evaluate. The human subjects

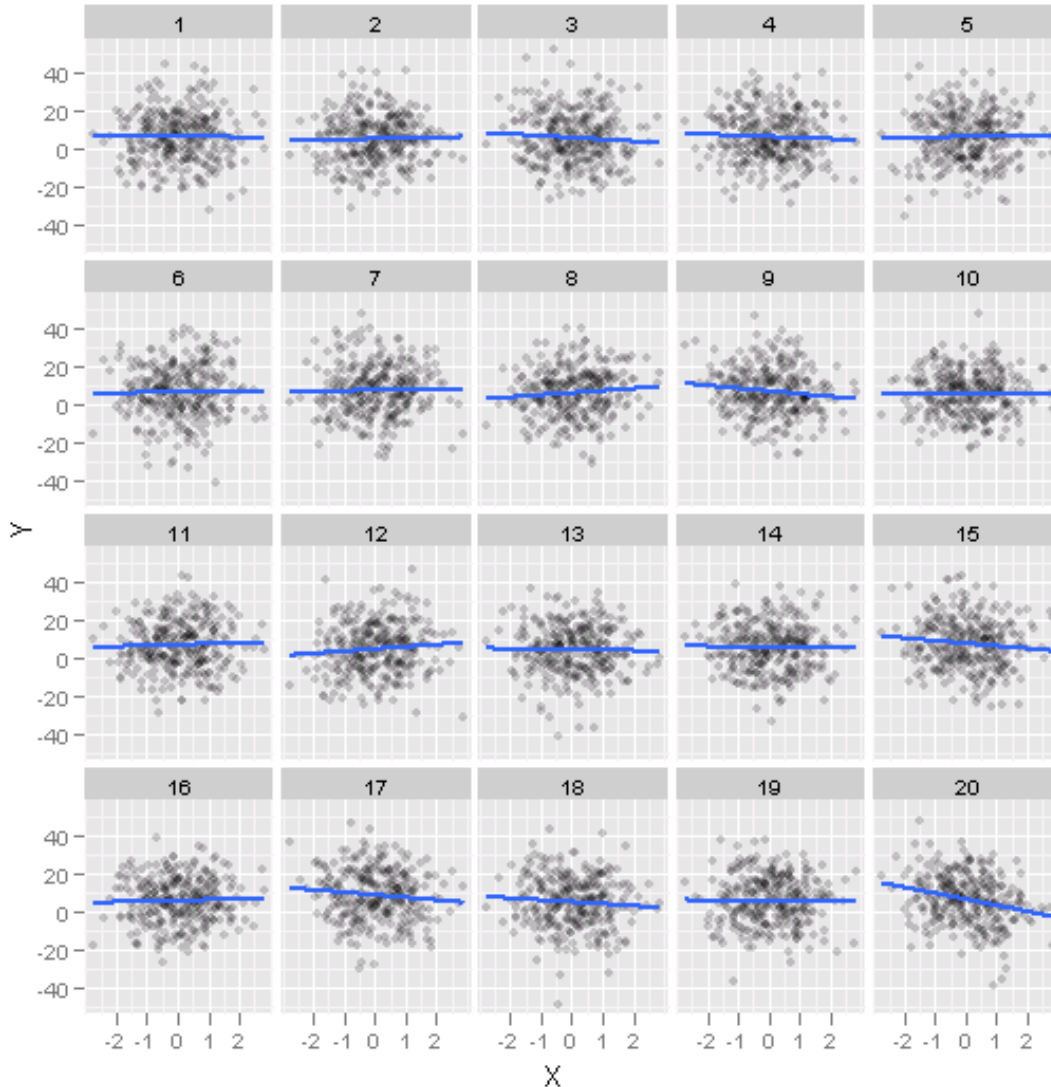


**Figure 2.1:** One of 70 lineups used in experiment 2 Majumder et al (2012). Of the 65 people who examined the lineup, 63 selected the data plot, which is in position 20.

were hired from Amazon Mechanical Turk where is a marketplace for work that requires human intelligence.

The controlled model in their first experiment is

$$Y_i = \beta_0 + \beta_1 X_{i1} + \beta_2 X_{i2} + \epsilon_i$$

where  $\beta_0 = 5, \beta_1 = 15, X_1 \sim \text{Poisson}(\lambda = 30), \epsilon_i \sim N(0, \sigma^2), i = 1, 2, \dots, n, \beta_2$  used in generating real data is specified in table 2.1. While in the null model  $\beta_2 = 0$ , and the null

data was generated by simulating from  $N(0, \hat{\sigma}^2)$ . This experiment was aimed to test the ability of human on detecting the effect of  $X_2$ .

Their second experiment is very similar to the first one, but there is only one continuous variable  $X_1$  on the right-hand side. It examined the performance of humans in recognising linear association between two variables, in direct comparison to conducting a  $t$ -test of  $H_0 : \beta_k = 0$  vs  $H_a : \beta_k \neq 0$  assessing the importance of including variable  $k$  in the linear model. The actual data model is

$$Y_i = \beta_0 + \beta_1 X_{i1} + \epsilon_i$$

where  $\beta_0 = 6$ ,  $X_1 \sim N(0, 1)$ , and the null data was generated from  $N(0, \hat{\sigma}^2)$ .

The third experiment in their paper contains contaminated data where the actual data were in fact generated from two different specifications.

$$Y_i = \begin{cases} \alpha + \beta X_i + \epsilon_i & X_i \sim N(0, 1) \quad i = 1, \dots, n \\ \lambda + \eta_i & X_i \sim N(\mu, 1/3) \quad i = 1, \dots, n_c \end{cases}$$

where  $\epsilon_i \sim N(0, \sigma)$ ,  $\eta_i \sim N(0, \sigma/3)$ ,  $\mu = -1.75$ ,  $\beta \in (0.1, 0.4, 0.75, 1.25, 1.5, 2.25)$ . And  $n = 100$ ,  $n_c = 15$ ,  $\alpha = 0$ ,  $\lambda = 10$ ,  $\sigma = 3.5$ . The null plots were generated from  $N(0, \hat{\sigma}^2)$ .

Other parameters in the “actual” data sets of Turk experiment one and Turk experiment two are shown in the table 2.1. In this study, we will mainly focus on the their second experiment and use its database to form our first comparison experiment. This experiment 2 utilized 70 lineups of size 20 plot, with varying degrees of departure from the  $H_0 : \beta_k = 0$ . There were 351 evaluations by human subjects. These results will be used for comparison with the deep learning model. An example lineup question in Turk experiment 2 is shown in Figure 2.1 (attached in Appendix). For this lineup, 63 of the 65 people who examined it selected the data plot (position 20) from the null plots. There is clear evidence that the data displayed in plot 20 is not from  $H_0 : \beta_k = 0$ .

**Table 2.1:** Combination of parameter values used for simulation in Turk's study.

Sample size (n)	Error SD(sigma)	Experiment 1 beta2	Experiment 2 beta1
100	5	0,1,3,5,8	0.25, 0.75, 1.25, 1.75, 2.75
100	12	1,3,8,10,16	0.5, 1.5, 3.5, 4.5, 6
300	5	0,1,2,3,5	0.1, 0.4, 0.7, 1, 1.5
300	12	1,3,5,7,10	0, 0.8, 1.75, 2.3, 3.5

## 2.2 Linear relationship simulation

The design for our model under the alternative hypothesis in the first experiment is similar to what Simchoni (2018) did in his blog. But the parameters are tailored to compare the computer performance with the Turk study results.

The model under the alternative is designed as:

$$Y_i = \beta_0 + \beta_1 X_i + \varepsilon_i, \quad i = 1, \dots, n$$

And all the parameters in our model were designed to cover the range used in the second experiment in Turk study (Majumder, Hofmann, and Cook, 2013). Therefore, the relevant parameters in our model are generated using the following specification.

- $X \sim N[0, 1]$

Distributions of X has an impact on the shape of the scatters. For instance, if X is generated from a uniform distribution, then the plots will look like a square when the sample size is large; while look like a circle if X follows a normal distribution.

- $\beta_0 = 0$

Intercept is arbitrarily set to be zero because it has no impact on the patterns in the data plots.

- $\beta_1 \sim U[-10, -0.1] \cup [0.1, 10]$

$\beta_1$  is designed to be uniformly generated from -10 to 10 (excluding -0.1 to 0.1).

- $\varepsilon \sim N(0, \sigma^2)$  where  $\sigma \sim U[1, 12]$

$\varepsilon$  is designed to be uniformly distributed from 1 to 12.

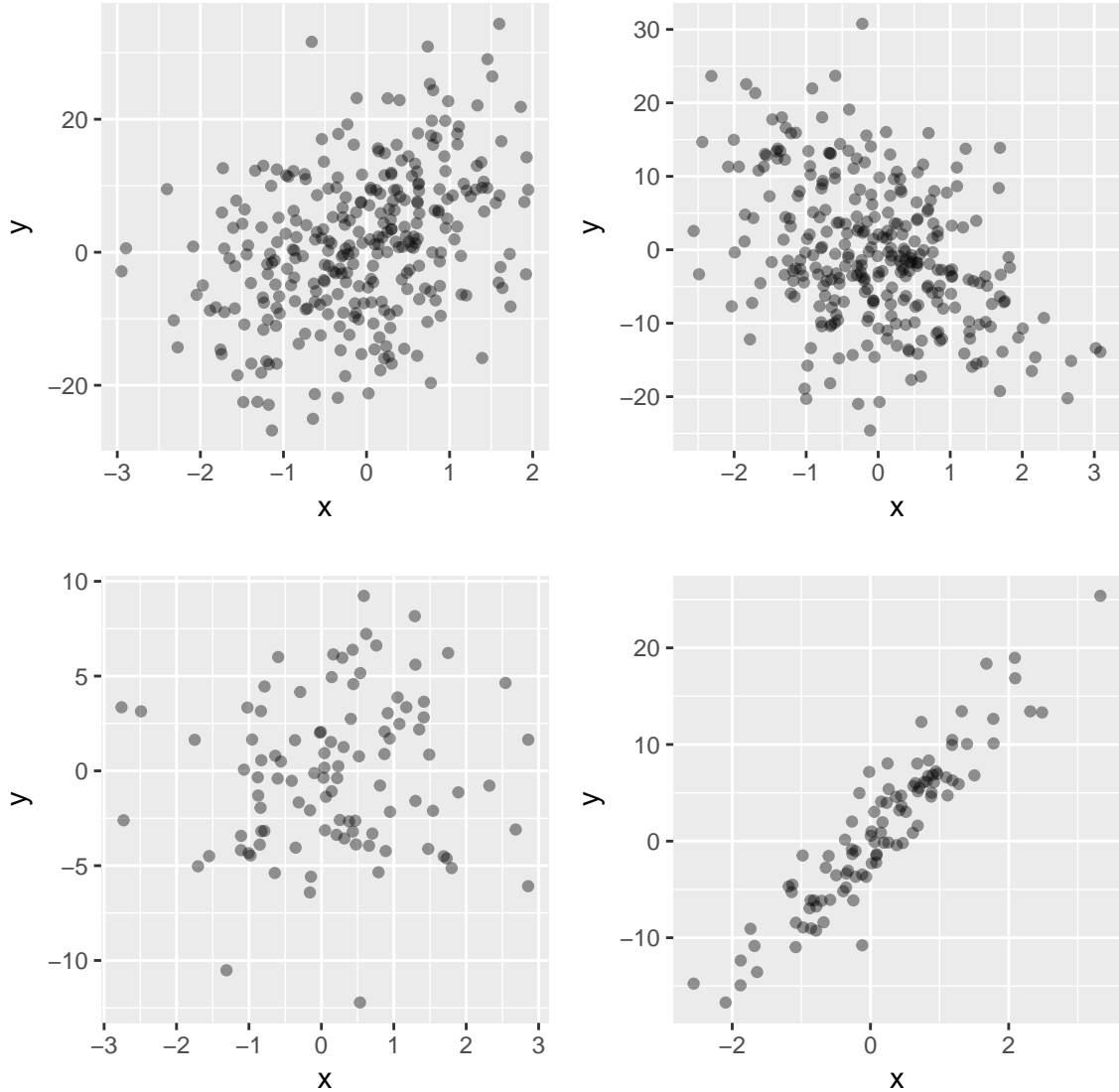


**Figure 2.2:** Four examples of data plots generated from the classic linear model.

- $n = U[50, 500]$

The sample sizes of each data set vary from 50 to 500 observations.

Figure 2.2 shows four example plots generated using the specifications above. To facilitate the computer vision, all texts, ticks and titles of X and Y axes are removed, so does the background grid. Under this controlled structure, a total number of 240,000 datasets are simulated. Figure 2.3 contains a histogram of the simulated  $n$ , a histogram of the simulated  $\beta$ , a histogram of the simulated  $\sigma$ , a histogram of the estimated sample p-value, a scatter plot of  $\beta$  against  $n$  and a scatter plot of  $\sigma$  against  $n$ . These plots show good coverage over the alternative parameter space.

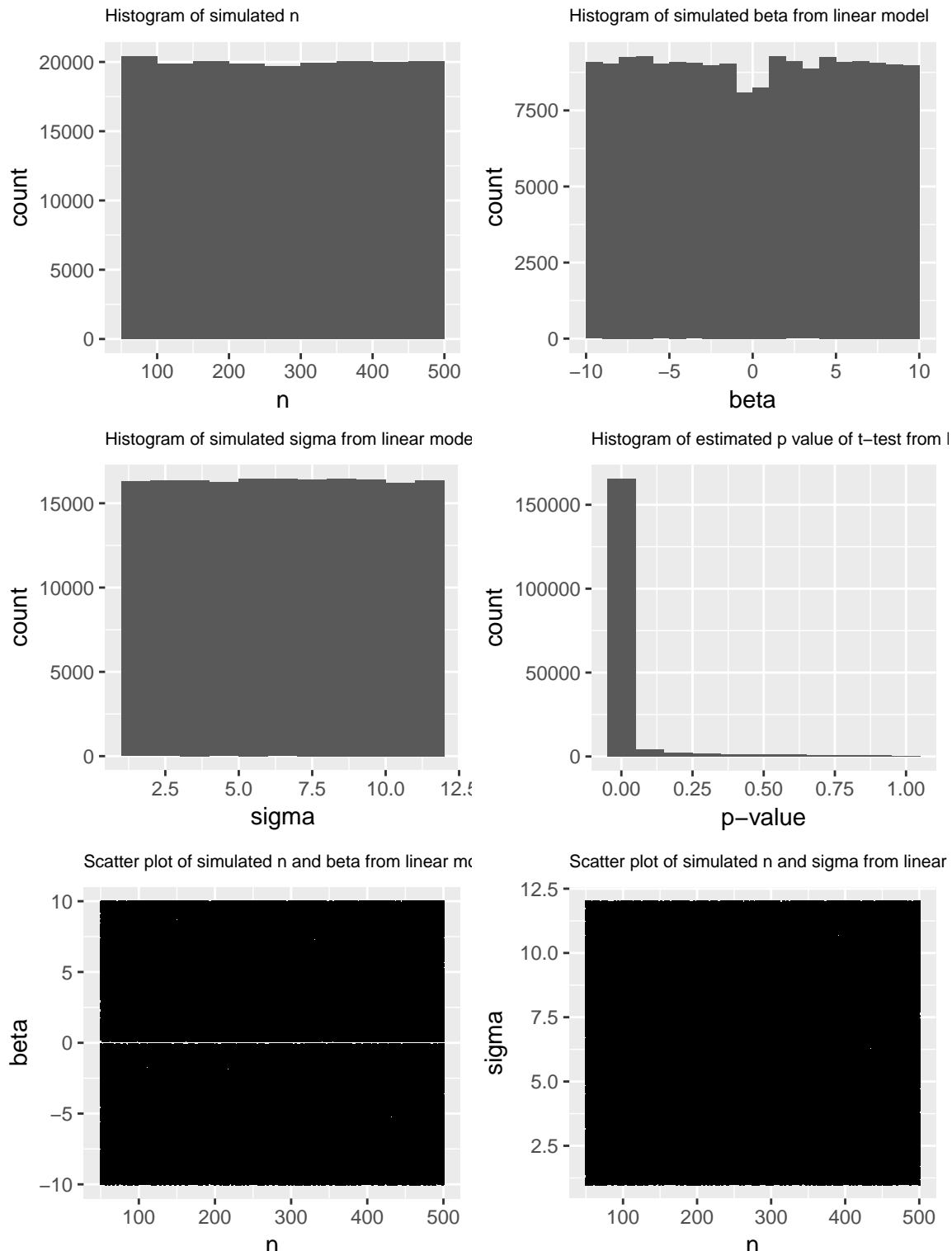


**Figure 2.3:** Overview of parameter values used in the linear class simulation, for computer model training. Good coverage is obtained across the parameter space.

## 2.3 Null plot simulation

This is the null scenario in our first experiment, eg. the two variables under tested are independent of each other. If the data arise from this situation, then the data plots will not show any systematic patterns theoretically. It is true that there must be some undesired patterns formed out of randomness, especially when the sample size is small. Unlike what Simchoni did in his post, no conventional tests will be used to sort out the “significant/insignificant” samples. Because the answer to the question that if the deep learning model can distinguish from patterns formed by chance and by nature is also interesting. The model is designed the same as the linear model:

$$Y_i = \beta_0 + \beta_1 X_i + \varepsilon_i, \quad i = 1, \dots, n$$

with elements of the model generated using the same specification as the linear model, except

$$- \beta_1 = 0$$

e.g. the coefficient of  $X_i$  is always zero. So  $X$  and  $Y$  are uncorrelated of each other.

Figure 2.4 are four example plots generated using the specifications above. Same as the linear model simulation, a total number of 240,000 datasets are simulated under this structure. Figure 2.5 contains a histogram of the simulated  $n$ , a histogram of the simulated  $\sigma$ , a histogram of the estimated sample p-value and a scatter plot of  $\sigma$  against  $n$ . These plots show good coverage over the null parameter space. All simulated data and associated parameters including estimated sample p-values of t-test are saved and are used later on for calculating the performance of conventional t-test.

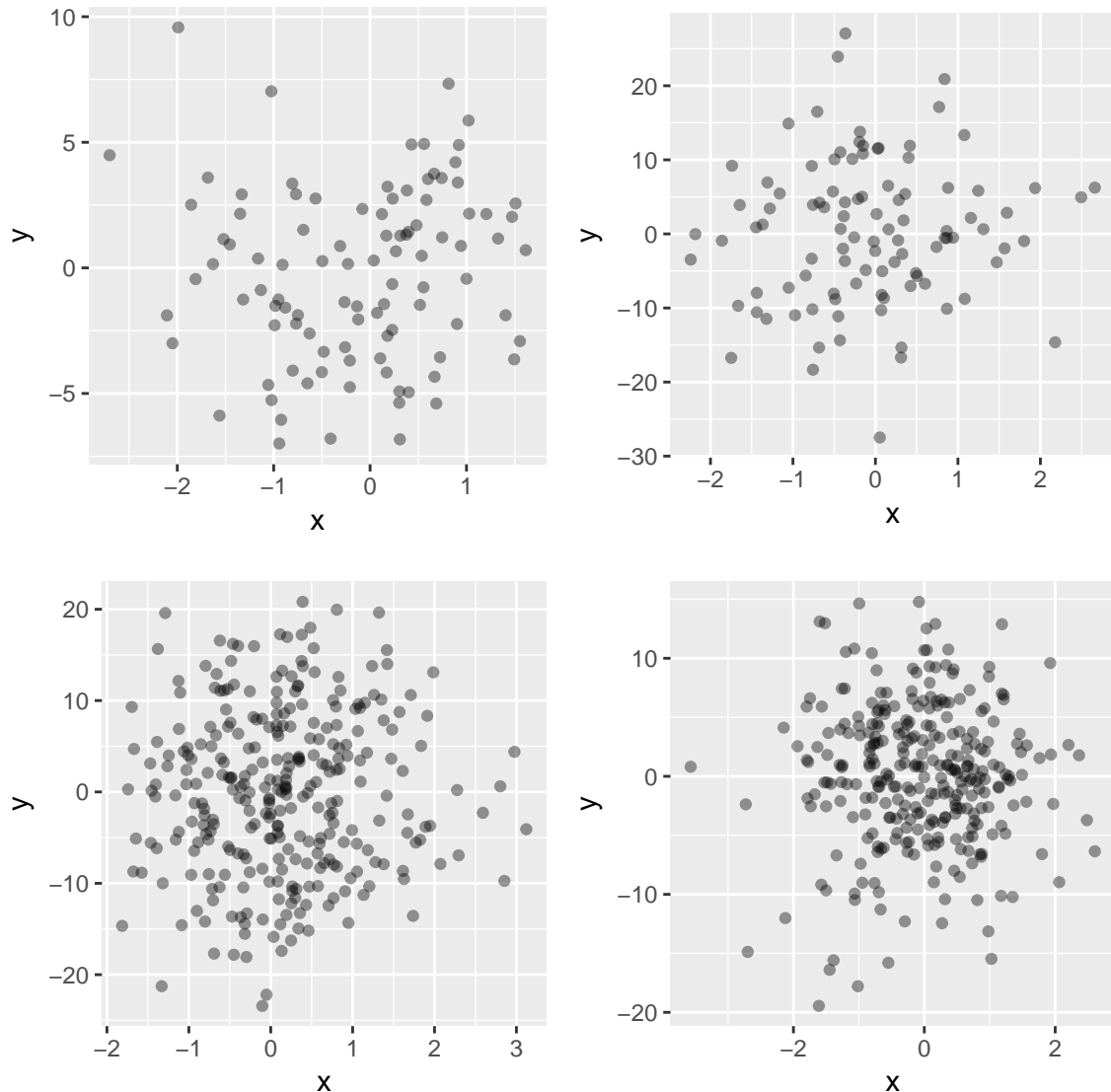


**Figure 2.4:** Four examples of data plots generated with two independent variables

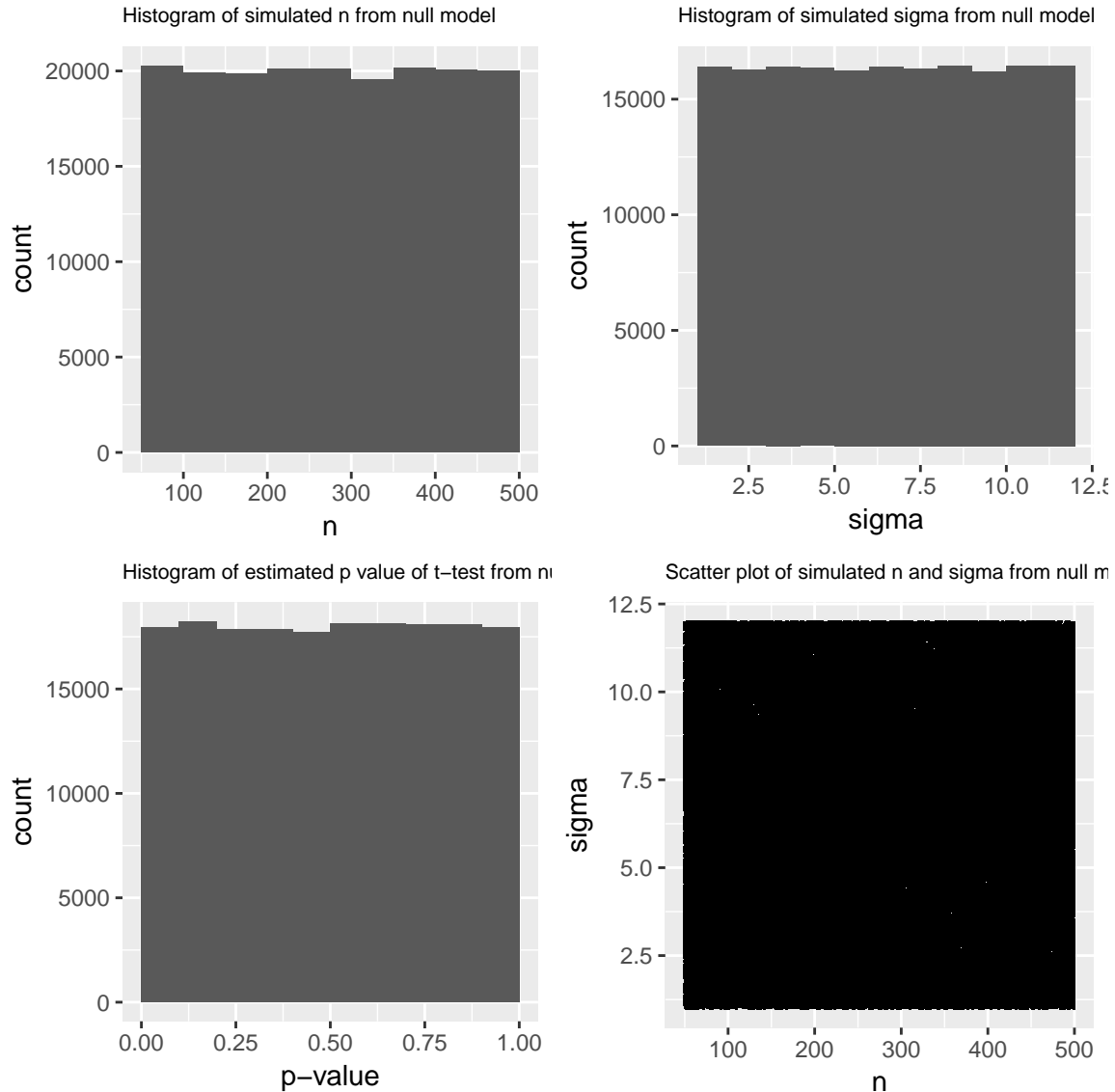


**Figure 2.5:** Overview of parameter values used in the null class simulation, for computer model training. Good coverage is obtained across the parameter space.

## 2.4 Computer model

All convolutional neural network related work is done by the Keras (Chollet et al., 2015) package in R (R Core Team, 2013), which interfaces to the python software. The plots used for training and testing in this section is the scatterplot between the dependent variable Y and the independent variable X. It can also be considered as the residual plot of such data fitting to a constant model. The R package ggplot2 (Wickham, 2009) is used to generate the plots. All plots are resized to  $150 \times 150$  pixel and saved as png. This size is similar to the plot size used in the lineup for human evaluation. As for the labels given to each image, we use the true population as the samples' identification directly.

As mentioned above, 240,000 data sets are generated for each of the two groups in the first experiment. 100,000 of them are set apart for training. Another 40,000 of the data sets are set apart as the validation set in order to monitor during training the accuracy of the model on data it has never seen before. And the leftover (100,000 data sets) become the unseen test set. We make the test set so large that we can compare the performance of the convnet with the conventional t-test properly.

“A convnets takes as input tensors of shape (image height, image width, image channels).”(Chollet and Allaire, 2018) The channels are normally equal to three for RGB. In our case, the input tensors are of shape  $150 \times 150 \times 1$ . The channel is equal to one because the input data is grayscale images. Therefore the convnet will be configured to process inputs of size  $(150, 150, 1)$ . We'll do this by passing the argument `input_shape = c(150, 150, 1)` to the first layer. The R codes below are used to build the convnets in R. From figure 2.6, the output shape changes after every layer of “conv” and “pooling” operations. The original  $150 \times 150 \times 1$  image is finally sliced into a  $7 \times 7 \times 128$  object (3D tensor). The figure 2.7 describes how “convolution” and “max pooling” operation works. By “convolution” the image matrix is multiplied by a filter, different filter gives different output matrix which extracting different features from the image. Max pooling select the max number within a certain area. Then we need to flatten these 3D tensor into 1D tensor so that they can be processed by the “sigmoid” function in the end. The “sigmoid” is, in fact, a special case of logistic function.  $S(x) = \frac{1}{1+e^{-x}}$ . From this model structure, we can also see that a total

number of 3,452,545 parameters need to be estimated, this is done by gradient descent. 10 epochs (1 epoch = 1 iteration over all samples) are done for training in our first experiment. The model specifications given by each epoch are saved, the one gives the overall highest accuracy is chosen to represent the computer.

```
library(keras)

model <- keras_model_sequential() %>%
  layer_conv_2d(filters = 32, kernel_size = c(3, 3),
                activation = "relu",
                input_shape = c(150, 150, 1)) %>%
  layer_max_pooling_2d(pool_size = c(2, 2)) %>%
  layer_conv_2d(filters = 64, kernel_size = c(3, 3),
                activation = "relu") %>%
  layer_max_pooling_2d(pool_size = c(2, 2)) %>%
  layer_conv_2d(filters = 128, kernel_size = c(3, 3),
                activation = "relu") %>%
  layer_max_pooling_2d(pool_size = c(2, 2)) %>%
  layer_conv_2d(filters = 128, kernel_size = c(3, 3),
                activation = "relu") %>%
  layer_max_pooling_2d(pool_size = c(2, 2)) %>%
  layer_flatten() %>%
  layer_dense(units = 512, activation = "relu") %>%
  layer_dense(units = 1, activation = "sigmoid")
```

The plot of the training history (figure 2.8) shows high accuracy achieved in both train and validation set (93%-94%); slight overfitting starts from the fourth epoch; the variation of the values of accuracy and loss in validation set are very small after the fourth epoch. Hence, both our convnets and dataset are large enough and the training of our first experiment can be concluded. Then we select the fourth, sixth, eighth and the tenth model to have them tested on the unseen test set. And the results are shown in the table 2.2. In this table, the “ $1 - \alpha$ ” means the accuracy of each computer model tested on the “null data” in the test set only.  $\alpha$  here is an analogy to the Type I error in the conventional hypothesis test.

Model

Layer (type)	Output Shape	Param #
conv2d_1 (Conv2D)	(None, 148, 148, 32)	320
max_pooling2d_1 (MaxPooling2D)	(None, 74, 74, 32)	0
conv2d_2 (Conv2D)	(None, 72, 72, 64)	18496
max_pooling2d_2 (MaxPooling2D)	(None, 36, 36, 64)	0
conv2d_3 (Conv2D)	(None, 34, 34, 128)	73856
max_pooling2d_3 (MaxPooling2D)	(None, 17, 17, 128)	0
conv2d_4 (Conv2D)	(None, 15, 15, 128)	147584
max_pooling2d_4 (MaxPooling2D)	(None, 7, 7, 128)	0
flatten_1 (Flatten)	(None, 6272)	0
dense_1 (Dense)	(None, 512)	3211776
dense_2 (Dense)	(None, 1)	513

Total params: 3,452,545  
 Trainable params: 3,452,545  
 Non-trainable params: 0

**Figure 2.6:** The deep learning model structure used for both of the experiments.

Similarly, the “power” is the accuracy of each computer model tested on the “linear data” in the test set only. The t-test performance in this table is calculated at 5% significance level.

The 8th model is chosen according to the overall accuracy on the test set. We should note that since the majority of the data plots in Turk’s experiment have been generated with linear relationship (when the alternative hypothesis is true), it is a disadvantage for the computer comparing in terms of being tested on the Turk’s data. Because of the difference in  $\alpha$  ( $\alpha \approx 0.02$  for the 8th computer model) the 5% significant t-test and 5% human evaluations may have higher power than the computer model.

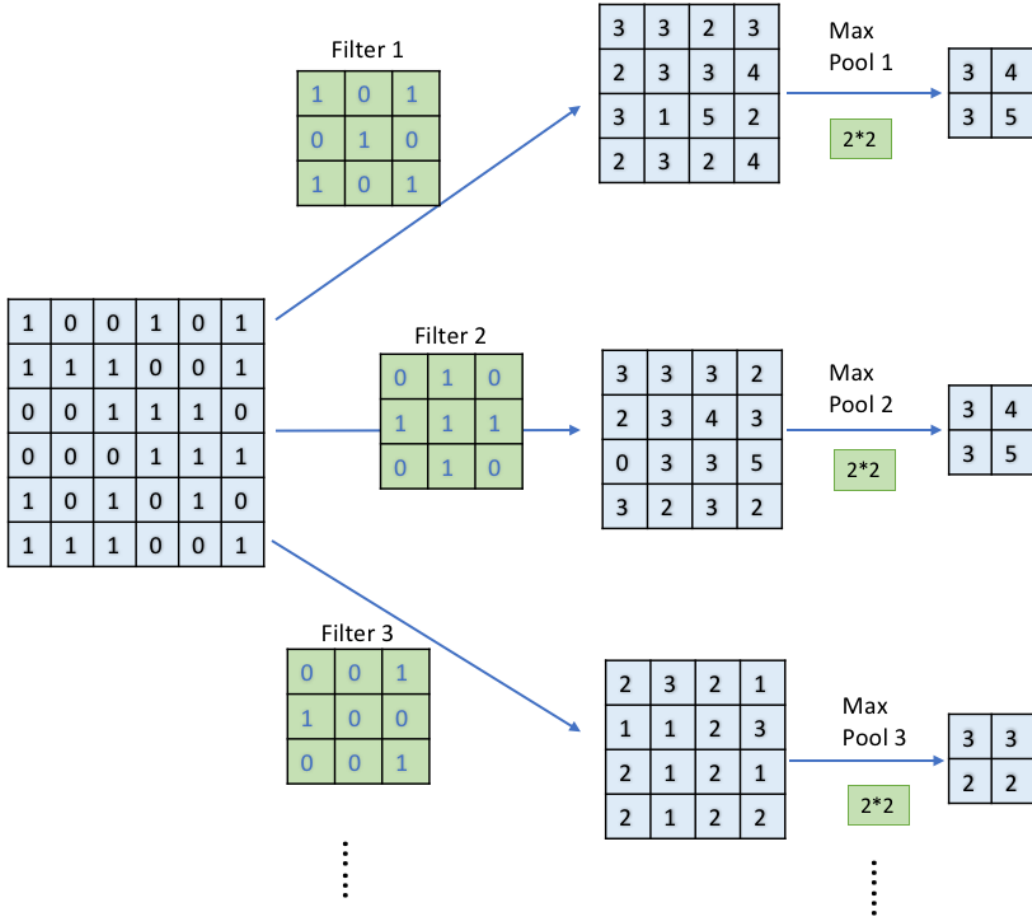


**Figure 2.7:** Illustration of convolution and pooling steps on an image. The convolution step applies a fixed number of filters to sliding windows of  $3 \times 3$  cells. Pooling applies a statistic to distinct  $2 \times 2$  tiling of the image. In our model, the statistic used is the maximum of the four values. These transformations are the pre-processing steps done on every image in the training sample, to fit the model, and also to the validation and test images prior to prediction.

Tests	Linear	Null	Overall
4 epoch	0.892	0.984	0.938
6 epoch	0.889	0.986	0.937
8 epoch	0.896	0.981	0.939
10 epoch	0.904	0.971	0.938
5% t-test	0.921	0.949	0.935

**Table 2.2:** Performance of four checkpoints from the convnets model, and the 5% significant t-test, computed on the test set. Accuracy is reported for each class, and overall. There is a slight improvement as the number of epochs increases, with 10 epochs being reasonably close to the ideal t-test accuracy.

## 2.5 Comparing results

The performance of the computer model for the Turk study data is tested in three steps:

- Re-generate the 70 “real plots” using the same data in Turk study (without null plots);
- Create a separate test directory for the 70 “real plots” exclusively;
- The computer model’s predicted accuracy over the 70 “real plots” is recorded as the model’s performance.

The conclusion of human evaluation is obtained differently from the computers. Because human evaluated “lineup”, not only the “real plots”. The performance is tested in five steps:

- Count the total number of evaluations made by human for one lineup ( $N$ ) and the number of correct answers for that lineup ( $k$ );
- Obtain  $N$  and  $k$  for all 70 lineups;
- Calculate p-value associated with each real plot using the formula introduced in section 2 of Majumder, Hofmann, and Cook (2013);
- Draw the conclusion: reject the null when the calculated p-value is smaller than  $\alpha$ .
- The accuracy of the conclusions the 70 real plots is presenting for the human performance.

For a fair competition, the Type I error ( $\alpha$ ) should be held the same for all test methods. However, we do not have direct control over the  $\alpha$  of the computer model. Because the  $\alpha$  estimated from the computer model is close to 2%. Therefore, 2% significant t-test and 2% significant human conclusion are also included to give a complete picture of the comparison. The comparing result (table 2.3) is interesting. Human achieves the highest accuracy, and the conclusion from the human evaluation is robust to smaller p-values; 5% significant t-test is the second best, 2% significant t-test and the computer model give the same results.

**Table 2.3:** Accuracy of testing the 70 data plots evaluated by human computer and the conventional t-test.

Rank	Tests	No. of correct	Accuracy
1	Human 5%	47	0.6714
1	Human 2%	47	0.6714
2	T-test 5%	43	0.6143
3	Computer 2%	39	0.5571
4	T-test 2%	39	0.5571

## 2.6 Aside discussion

Under the condition specified in this chapter, the conventional t-test is supposed to be the uniformly most powerful (UMP) test in terms of detecting the linear relationship according to the Neyman–Pearson lemma. Although human achieved the best performance in the Turk experiment dataset, it does not mean computer does badly since the Turk experiment dataset only contains 70 plots. As we can see from table 2.2, t-test and convnets behave quite similarly on both the test data and Turk’s experiment data. Given our test set is large enough (200,000 images totally), it is reasonable to assume that the convnets is, in fact, implementing the t-test or trying to approach the t-test. In other words, the best strategy the convnets learned, in this case, may turns out to be t-test.

To check this idea, we calculated the accuracy of t-test again, with different  $\alpha$  (from 0.005 to 0.1 with 0.005 increments) on all 200,000 test sets. The estimated power and overall accuracy were recorded. When  $\alpha = 0.015$ , the overall accuracy reaches its maximum. This value approximately coincide with the  $\alpha$  chosen by the convnets. And since the  $\alpha$  of convnets is from 0.0142 to 0.0347 on the test set, we truncated the t-test data to create figure 2.9. The upper dots represent overall accuracy achieved by convnets (red) and t-test (green), while the lower dots stand for the estimated power in the test set. The smooth line overlaid aids the eye in seeing patterns. From this graph, we can see the convnets and t-test perform very similarly, while t-test has overall better performance.

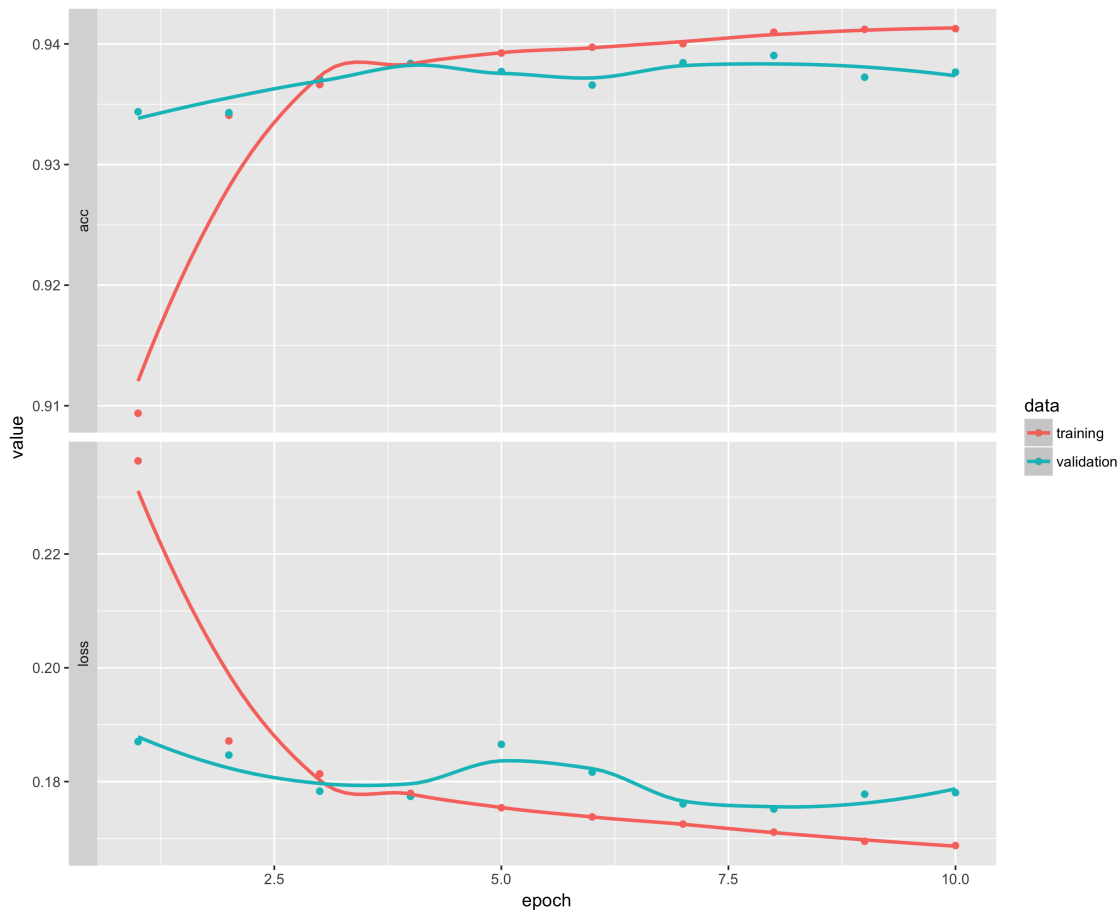


**Figure 2.8:** Training and validation metrics of linear vs. null model in our first experiment. The top plot is the accuracy achieved in train and validation sets, while the bottom plot is the loss. Red presents model performance in train set while green presents validation.

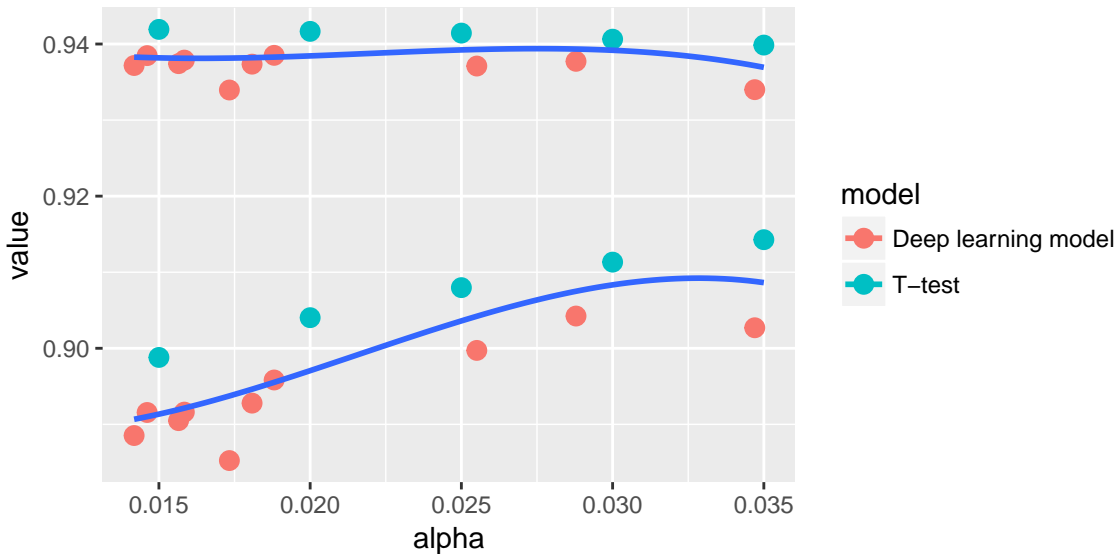


**Figure 2.9:** Comparison between computer model and t-test for alpha in (0.01, 0.04), they perform very similarly, but t-test has overall better performance.

## **Chapter 3**

# **New experiment comparing human vs. computer on reading heteroskedasticity**

Turk experiment mainly considers linear data; we extend their study by including heteroscedasticity in this paper. A new database of human evaluating heteroskedasticity is created by a small experiment. This new database is used to compare the performance of the computer model, the convnets. The convnets is trained on the same parameter simulation framework and tested on the same data as the human evaluations.

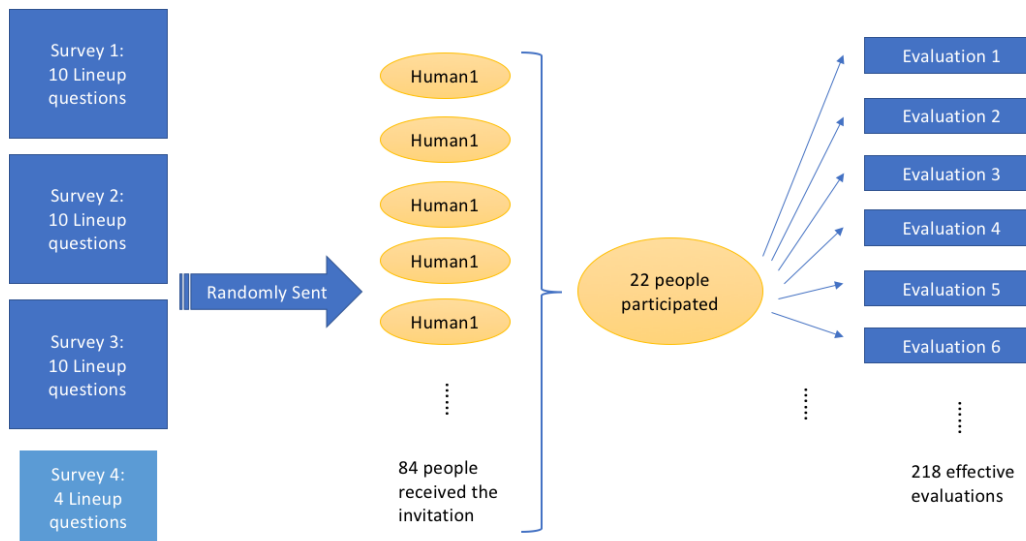


**Figure 3.1:** Human subject experiment set-up for the second hypothesis test. Four surveys were sent to 84 people, 22 participated, 218 effective evaluations were collected.

### **3.1 A new human experiment**

The experiment is to evaluate the human ability to read heteroskedasticity from residual plots. It is rendered at Monash University, Melbourne Australia. The participants are all students or lecturers in the department of econometrics and business statistics.

Four surveys were randomly sent to 84 people by email, three of the survey consists of ten lineup questions, and the fourth survey has only four lineup questions. All lineup questions are of size 20 plot and are designed to have different difficulty levels. Only one lineup question appears in the survey twice, thus, we have  $33 (10 \times 3 + 4 - 1)$  distinct questions in total. A total number of 22 people have participated. Five people evaluated two surveys. One people selected four plots for each lineup by accident, this person's response was removed from the data. In summary, we collected 218 effective evaluations from 21 people. Figure 3.2 is an example of the lineup used as a question in the survey. The “real plot” and “null plot” data in all lineup questions was simulated using the same specifications given in the next two sections respectively.

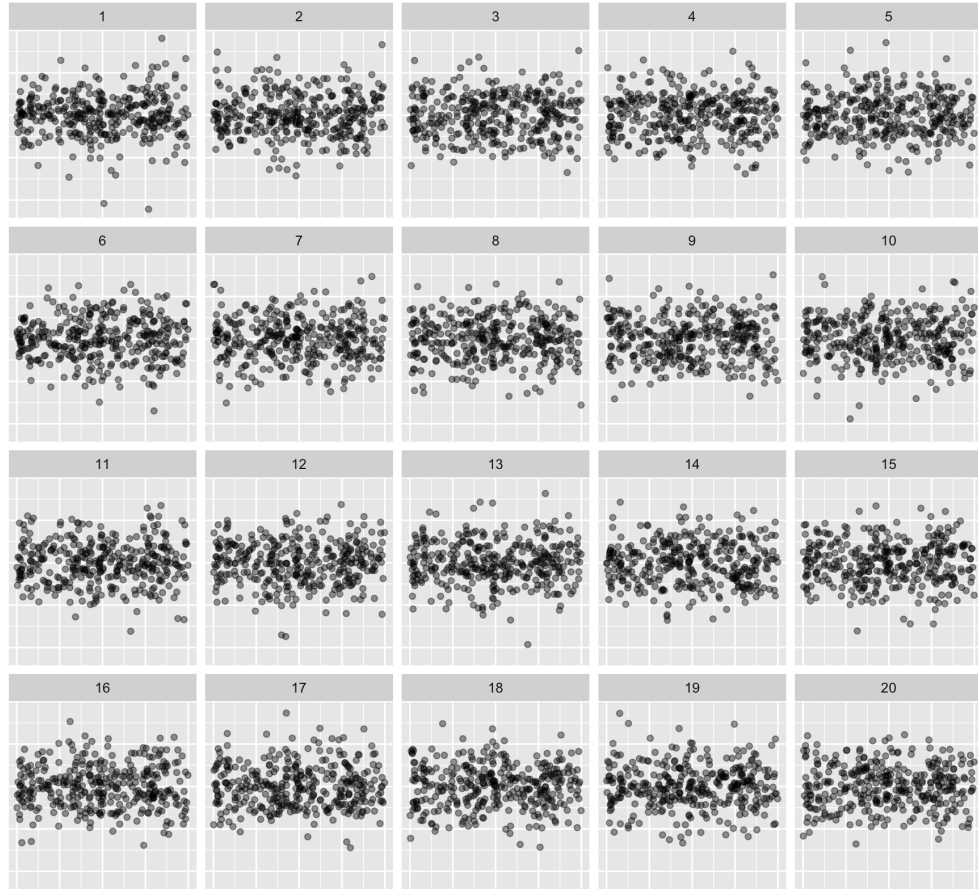


**Figure 3.2:** An example question in the survey, 4 out of 6 people picked the real plot, the real plot is the first one.

## 3.2 Heteroskedasticity simulation

A linear model with heteroskedasticity is the model implied in the alternative hypothesis of the second experiment in this paper, where the constant variance assumption of the linear model is violated while all other conditions are met. By the definition given in Wooldridge (2015), “The homoskedasticity states that the variance of the unobserved error,  $u$ , conditional on the explanatory variables, is constant. Homoskedasticity fails whenever the variance of the unobserved factors changes across different segments of the population, where the segments are determined by the different values of the explanatory variables.” There are countless types of heteroskedasticity since the “change of the variance” could be related to “the explanatory variables” in various ways. It is not feasible to list out all kinds of heteroskedasticity by a single function. For simplicity, we will focus on one example of them, a linear correlation between the explanatory variable  $X$  and the standard deviation

of the error term. Hence the relationship between the explanatory variable X and the variance of the error term will be quadratic. The results of this experiment though can be generalized to more complicated cases.

The model structure is the same with the classic linear model:

$$Y_i = \beta_0 + \beta_1 X_i + \varepsilon_i, \quad i = 1, \dots, n$$

with elements of the model generated by the following processes

- $X \sim U[-1, 1]$  To better present the heteroskedasticity in the data, a uniform distribution of X is used instead of normal distribution. The range is set to be small (from -1 to 1) in order to balance the data with weak heteroskedasticity appearing more frequently.
- $\beta_0 = 0$  Intercept is set to be zero. Because the residual plot but not data plot is used in this experiment. Therefore, the information contained in  $\beta_0$  will be extracted by the linear regression we fit to the data.
- $\beta_1 \sim U[0.5, 1]$   $\beta_1$  has little impact in this case as well so it is set to be uniformly generated from 0.5 to 1.
- $\varepsilon \sim N(0, (ax + v)^2)$  The variance of the error term is a quadratic function of the explanatory variable which controls the magnitude of heteroskedasticity in the model.
- $a \sim U(-5, -0.05) \cup (0.05, 5)$  The parameter a here, following uniform distribution from -5 to 5 (excluding -0.05 to 0.05), is the correlation coefficient between X and the standard deviation. Larger a gives stronger heteroskedasticity. This range is wide enough for our purpose.
- $v \sim N(0, 1)$  This new error term is added to the variance of  $\varepsilon$  so the relationship between the data can be more flexible.
- $ax + v - \min(ax + v)$  when  $\min(ax + v) < 0$  To keep the simulated standard deviation positive, and to keep the structure of the relationship between X and the residuals, the  $\min(ax + v)$  is subtracted from  $ax + v$  whenever the former is negative.

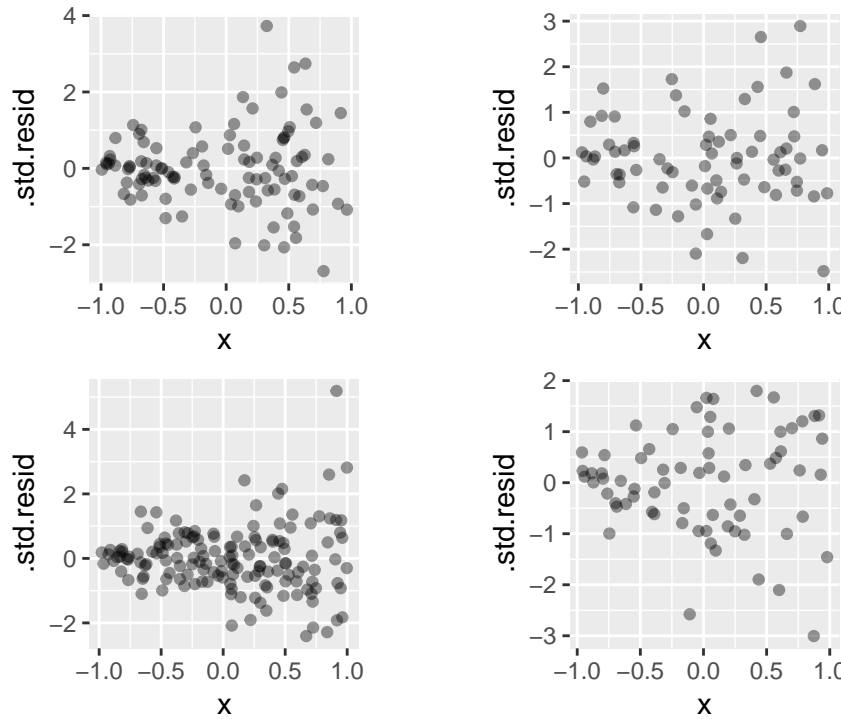


**Figure 3.3:** Four examples of residual plots generated from the linear model with heteroskedasticity

- $n \sim U[50, 500]$  The sample sizes are randomly generated from 50 to 500 to provide reasonable variations.

In general, the choice of the parameters is an empirical work. Primarily, we want the residual plots to show more variation; on the other hand, we need to limit the range of these parameters in order to keep the key features in the data. Figure 3.3 shows four examples of residual plots generated under this structure.

### 3.3 Null plot simulation

The null scenario in this experiment is the classic linear model. The model structure is the same as the heteroskedasticity one. When we simulate this data, we kept most of the parameters as the same with the alternative data and only changed the key feature of the error term. So the difference in this data set is:

- $\varepsilon \sim N(0, c)$
- $c = \text{mean}(ax + v)$

where  $c$  is a constant which equals to the mean of the  $ax + v$ . All other parameters in the null data are the same as the heteroskedasticity data.

### 3.4 White test

To provide a reference level of how computer and human are performing, a special case of the White test is used in this experiment. Every data set simulated from this section has been tested by this White test. The procedure of the White test (Wooldridge, 2015) is:

- Estimate OLS model for the data, obtain residuals ( $\hat{u}$ ) and the fitted values ( $\hat{y}$ ). Computer the squared OLS residuals ( $\hat{u}^2$ ) and the squared fitted values ( $\hat{y}^2$ ).
- Run an auxiliary regression as  $\hat{u}^2 = \eta_0 + \eta_1\hat{y} + \eta_2\hat{y}^2 + error$ , obtain the R-squared  $R_{\hat{u}^2}^2$ .
- Calculate the LM statistic which follows  $\chi^2_2$  distribution.
- Conclude based on p-values given certain  $\alpha$ .

We think this test is suitable for detecting the heteroskedasticity specified in this section, because  $\hat{y}_i = \hat{\beta}_0 + \hat{\beta}_1 x_{i1}$ , so the squared fitted value  $\hat{y}^2$  contains both the squares of the independent variable  $x^2$  and  $x$  itself. This form is consistent with our model design where the variance of error term is a quadratic function of  $x$ .

### 3.5 Computer model

In this experiment, a linear model first fit to the data. Residuals from the fitted model are standardized and extracted. The residual plot is made of standardized residuals against X. The convnets has the same structure as in the first experiment, and all hyper-parameters in this model are exactly the same as the previous one. Fifteen epochs are done in this experiment. All fifteen convnets models are saved. The training and validation metrics are shown in figure 3.4. The overfitting issue is again not severe in this case. The variation in accuracy and loss are very small even since the beginning. We believe the training data and the convnets are both large enough, and the model is well trained. Then the

fourth, eleventh and fifteenth epoch models are selected to be tested on the test set and the accuracy is shown in table 3.1. The 11th model is chosen to represent computer for the competition according to the overall accuracy. It is also worth noting that the  $\alpha$  (error rate in the null dataset) chosen by the convnets is between 1.6% to 3.3%, which is smaller than 5%; what's more, the power of the convnets (accuracy in the real dataset) is much higher than the white test. Therefore, the overall accuracy of the convnets is higher than the white test.

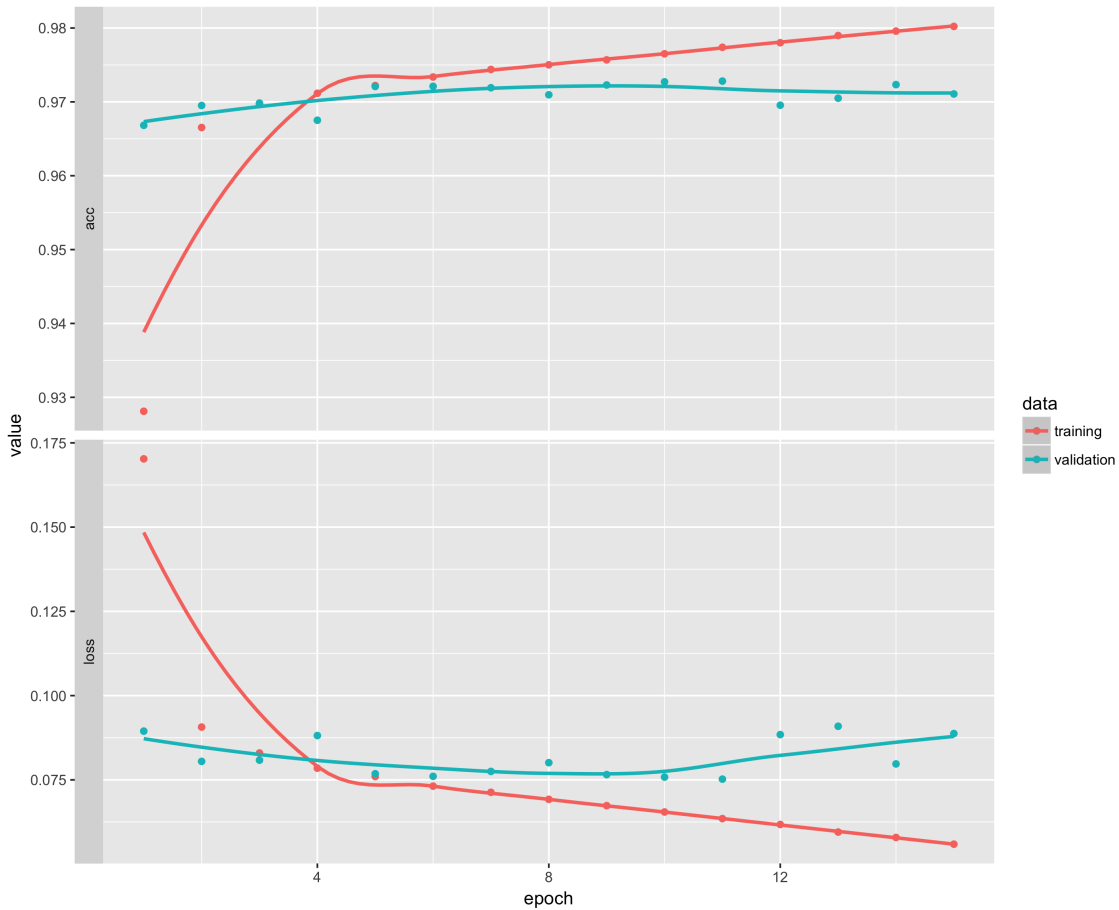


**Figure 3.4:** Training and validation metrics of heteroskedasticity vs. null model in our second experiment

	Tests	Heter	Homo	Overall
4 epoch	0.970	0.967	0.968	
11 epoch	0.963	0.984	0.974	
15 epoch	0.959	0.984	0.972	
5% White test	0.856	0.952	0.904	

**Table 3.1:** Performance of three checkpoints from the convnets model, and the 5% significant white-test, computed on the test set. Accuracy is reported for each class, and overall.

### 3.6 Comparing results

The performance of computer and human are computed by the same methods stated in chapter 2. The final competition dataset is the twenty-seven “real plots” used in the four surveys. Figure 3.5 displays the relationship between the proportion of correct answers for each question against the value of the simulated “ $a$ ” for the real plot in that lineup question. The proportion is increasing as the absolute value of “ $a$ ” increases. This meets our expectation since the value of “ $a$ ” controls the magnitude of “heteroskedasticity”. The stronger the relationship is in the data, the more people are able to pick the real plot.

Table 3.2 presents the accuracy achieved by our convnets, human and the white test for testing heteroskedasticity in those twenty-seven real plots. Different from the first experiment, this time the convnets achieves the best performance against human and the white test. In addition, the accuracy achieved by the convnets is also much higher than its competitors.

rank	tests	correct	accuracy
1.00	Computer 2%	25.00	92.59%
2.00	Human 5%	17.00	62.96%
2.00	White-test 5%	17.00	62.96%
3.00	White-test 2%	16.00	59.26%
4.00	Human 2%	15.00	55.56%

**Table 3.2:** Accuracy of testing the 27 data plots evaluated by human, computer and the conventional white-test.

### 3.7 Aside discussion

Our original design was to have three surveys of size ten questions and to include two “all-null” lineup questions per survey. By “all-null”, it means the “real plot” in that lineup was also generated from the null distribution. People were expected to having difficulties picking the real plot in that situation. However, because of one mistake we made in the data simulation procedure, the variance of the error terms associated with the real plots in the all-null lineups was not a single constant but a series of random numbers. Even if this series of random numbers had no relationship with the independent variable  $x$ , they led to undesired patterns in the data such as non-linearity and extreme outliers. Hence many

participants picked the real plot successfully for the six all-null lineup questions. To fix this issue, we had to remove the information related to the six all-null questions and made one extra survey to collect more data. This was the reason why we made three normal surveys plus an extra small one.

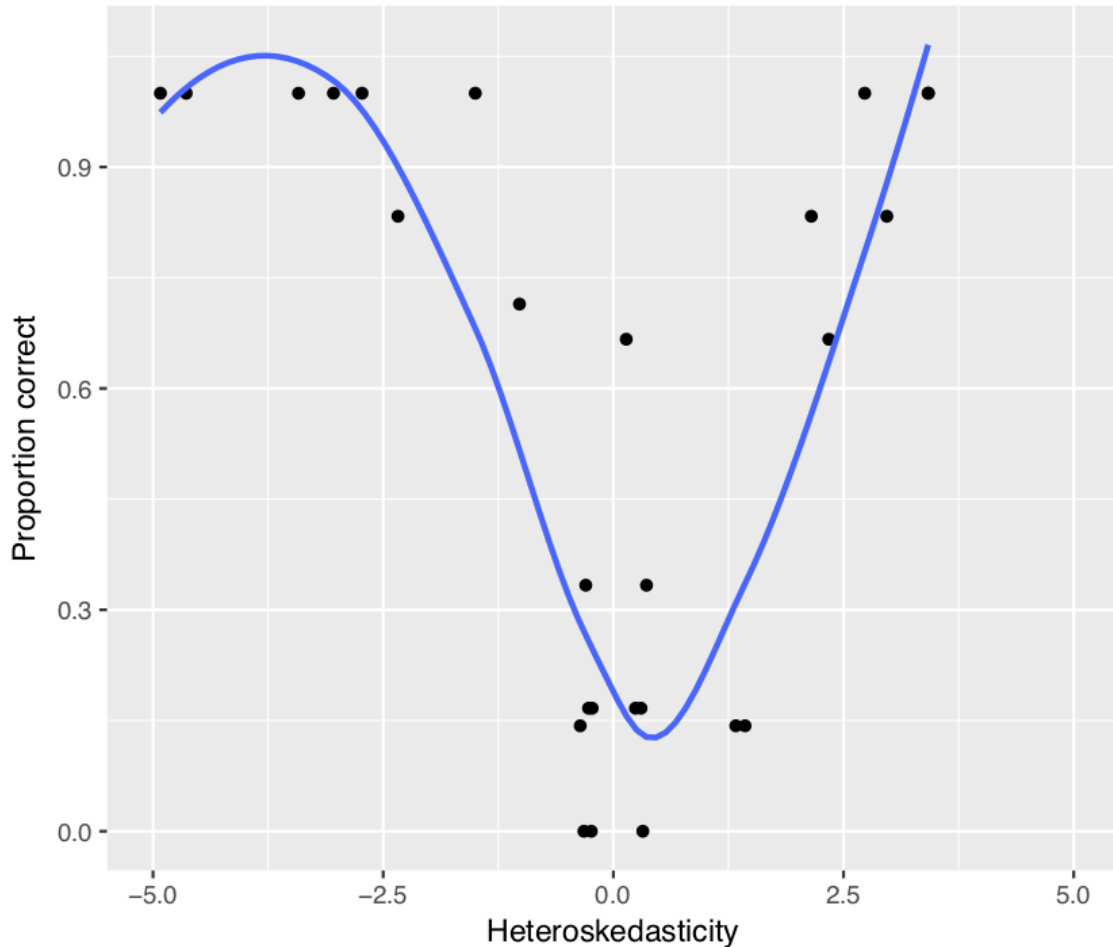


**Figure 3.5:** Proportion of correct answers for each lineup question against the simulated correlation "a" from human evaluation



## **Chapter 4**

# **Conclusion and discussion**

In summary, the convnet can be trained to perform similarly to human perception when the structure in the residual plots is very specific. Performance of convnets on the linear vs no structure is comparable to the human subjects' results; performance on detecting heteroskedasticity is better than the human subjects' results. Performance of the convnet is a little bit below the results obtained by the *t*-test for the linear experiment, but much higher than the white-test for the heteroskedasticity experiment.

As for the time needed for computer training, since a large number of images are employed in this study, and we rely only on the CPU, 10-20 hours is required for generating and saving all images, another 10-20 hours will be necessary for convnets model to be trained and tested. With an NVIDIA GPU, this duration will be shortened significantly.

Although this study has shown that the computer model, more specifically, the convnets is able to approach the best test (*t*-test) in detecting linear relationships from the null, the white test we used in the second experiment is too general to draw such meaningful conclusion. Because that white test is not the uniformly most powerful test under that specific condition. It is possible that a more powerful test, which is customized to the structure designed in our second experiment, can achieve higher accuracy than the convnets. However, this study gives hope to the future utilization of convnets in reading the residual plot. Unlike the conventional distribution tests, convnets does not require convoluted mathematical derivations and can be applied to any visualizable problems.

As a non-parametric inference method, what's more, convnets is not restricted to be valid under any assumptions, it is valid whenever there are distinguishable patterns in the residuals. Compared to human, the convnets is more stable in that it always gives consistent prediction once it is well trained while different groups of people may have different opinions on one plot. In addition, the computer training and testing can be done by a single computer which barely costs anything (other than our genuine efforts) while human evaluations could be much more expensive.

On the other hand, the computer also has pitfalls. Its ability is limited to the patterns provided by the training. The more patterns we want the convnets to recognize, the more structures we need to feed it. As for the future study, more types of structure could be considered, for example, other types of heteroskedasticity, the non-linear relationship, outliers, etc. The binary classification can also be extended into a multiclass classification, e.g. one convnets can be trained to recognize several departures from the null. What's more, to provide a more reliable comparison between human and computers, a larger human experiment is required. For an even further step, the convnets can be designed for even more general hypothesis testing purposes, the biggest challenge would be finding the most appropriate plot (the test statistic) which can show the key features for certain tests. For instance, if we are interested in telling a time series data with unit root from a trend stationary one, the most suitable plot may be the time plot.

# Bibliography

- Anscombe, F (1973). Graphs in Statistical Analysis. *The American Statistician* **27**(1), 17–21.
- Cairo, A (2016). “Download the datasaurus: never trust summary statistics alone”. Personal blog.
- Chollet, F et al. (2015). *Keras*. <https://keras.io>.
- Chollet, F and J Allaire (2018). Deep Learning with R.
- Culurciello, E (2017). The history of neural networks.
- Majumder, M, H Hofmann, and D Cook (2013). Validation of visual statistical inference, applied to linear models. *Journal of the American Statistical Association* **108**(503), 942–956.
- Majumder, M, H Hofmann, and D Cook (2014). Human factors influencing visual statistical inference. *arXiv preprint arXiv:1408.1974*.
- Matejka, J and G Fitzmaurice (2017). Same stats, different graphs: generating datasets with varied appearance and identical statistics through simulated annealing. In: *Proceedings of the 2017 CHI Conference on Human Factors in Computing Systems*. ACM, pp.1290–1294.
- R Core Team (2013). *R: A Language and Environment for Statistical Computing*. R Foundation for Statistical Computing. Vienna, Austria. <http://www.R-project.org/>.
- Simchoni, G (2018). “Applying deep learning for the visual inference lineup protocol”. Personal blog.
- Wickham, H (2009). *ggplot2: Elegant Graphics for Data Analysis*. Springer-Verlag New York. <http://ggplot2.org>.
- Wickham, H, D Cook, H Hofmann, and A Buja (2010). Graphical inference for infovis. *IEEE Transactions on Visualization and Computer Graphics* **16**(6), 973–979.
- Wooldridge, JM (2015). *Introductory econometrics: A modern approach*. Nelson Education.